



Performance analysis of series: shunt configuration based RF MEMS switch for satellite communication applications

P. Ashok Kumar¹ · K. Girija Sravani^{1,2} · B. V. S. Sailaja¹ · K. V. Vineetha¹ · Koushik Guha² · K. Srinivasa Rao¹

Received: 13 December 2017 / Accepted: 13 April 2018 / Published online: 11 May 2018
© Springer-Verlag GmbH Germany, part of Springer Nature 2018

Abstract

In this paper the RF-MEMS switch with series–shunt configuration on a single quartz substrate is presented to achieve high isolation than the individual series or shunt switches. This paper presents the isolation of series–shunt configuration switch of 84.7 dB is achieved at 26 GHz when both switches are in OFF state which is higher than the OFF state of the individual series switch and shunt switches. The return loss (S_{11}) is less than -60 dB, insertion loss is less than -0.09 dB is observed for better performance in satellite communication applications. The series/ohmic and shunt/capacitive membranes are designed with uniform spring structure and crab leg structure, respectively and simulated using FEM tool. Ashby's method is used to select the materials for the switch membranes/beam and dielectric layer. The gap between the dielectric and the movable beam is maintained at $3 \mu\text{m}$ in series switch and $2.5 \mu\text{m}$ for shunt switch to achieve same pull-in voltage of 23.5 V. The up-state and down-state capacitance of the device is calculated and compared with the simulated results which are 0.24 and 14.2 fF, respectively by considering TiO_2 as a dielectric layer between membrane and lower electrode.

1 Introduction

Radio frequency MEMS switches are very much used instead of the traditional gallium arsenide switches, field effect transistors and photo-injection-diode switches in RF and microwave systems, because of very low power dissipation and consumption, high isolation, low insertion and return losses, less cost and low weight (Rebeiz 2003). Surface micro-machining processes is used to fabricate the MEMS switches which consists of a very thin metallic membrane called as bridge (two end fixed beam) which regulates the transmitting of the electronic signal by mechanical deflection of the bridge over the electrode. The

different actuation techniques such as electrostatic (Muldavin and Rebeiz 2000a, b; Pacheco et al. 2000), electromagnetic (Yao et al. 1999), piezoelectric (Ruan et al. 2001) and thermal (Lee et al. 2009) actuation are used to actuate the MEMS switch. Electrostatic actuation is widely used because of negligible power consumption and linearity of the device. Switching operation is achieved by generating an electrostatic force between switch membrane and lower electrode. MEMS switches suffers low switching speed, high actuation voltages in RF circuits. (Daneshmand et al. 2009). A compact structure of Rotary electrostatic comb-drive actuators as a drive mechanism of the switch which operates in three state offers high isolation of -60 dB at 40 GHz. (Ikkechi et al. 2017) A high-force and high isolation metal-contact RF MEMS switch has been proposed to increase the isolation of the switch and got -36 dB at 10 GHz. (Deng et al. 2017) A novel laterally and micro-electro-thermally actuated RF MEMS switch is presented to have the isolation of -20 dB at 100 GHz (Zolfaghari et al. 2018).

This paper presents an approach to increase the isolation by considering series–shunt configuration RF MEMS switch arranged over the substrate made up of quartz, and with dielectric medium TiO_2 ($K = 100$). The devices results in excellent RF performance with high isolation and

✉ P. Ashok Kumar
puliashok9915@gmail.com

✉ K. Srinivasa Rao
srinivasakarumuri@gmail.com

¹ MEMS Research Center, Department of Electronics and Communication Engineering, Koneru Lakshmaiah Education Foundation (Deemed to be University), Green Fields, Vaddeswaram, Guntur 522502, India

² National MEMS Design Center, Department of Electronics and Communication Engineering, National Institute of Technology, Silchar 788010, Assam, India

low insertion loss characteristics. The series and shunt membranes are designed at same actuation voltage for electrostatic operation. The Electromechanical, pull-in voltage, spring constant and stress distribution and RF performance analysis is carried out using finite element modeler (FEM) tool.

The rest of the paper is organized as follows, in Sect. 2, the design of the proposed RF MEMS switch is discussed with the device structure of both capacitive and shunt membrane, working principle and its specifications and material selection for the switch. In the Sect. 3, various results such as stress distribution analysis, spring constant, pull-in voltage, C_d and C_u ratio analysis and switching response of the switch has been discussed. In Sect. 4, the RF performance characteristics such as insertion and return losses in ON state and isolation losses in OFF state have been discussed.

2 Theory

2.1 Device structure and working principle

The proposed MEMS switch consists of a Coplanar Wave guide which transmits the RF signal, dielectric layer made up of TiO_2 ($K = 100$) over the Quartz substrate. The actuation voltage is required to ON the series membrane and OFF the shunt membrane of the switch simultaneously. The coplanar wave guide consists of signal line with

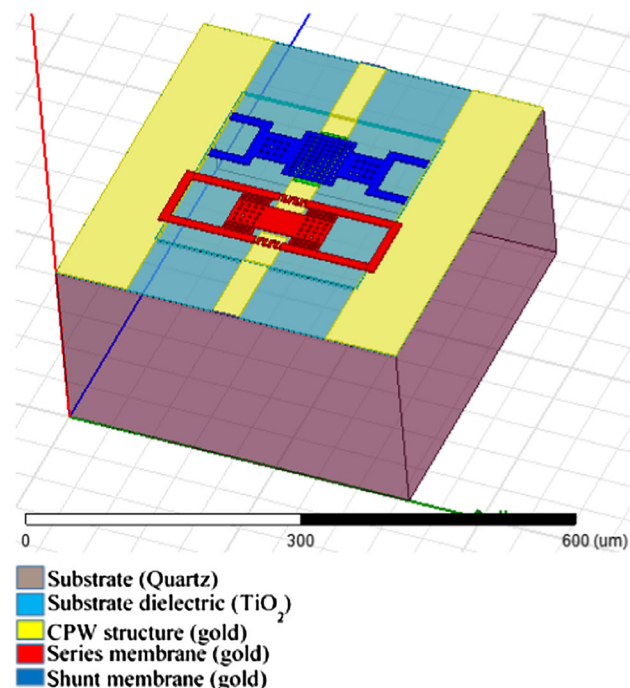


Fig. 1 Series–shunt configuration RF MEMS switch

$31.5 \mu\text{m}$ width and having a gap of $126 \mu\text{m}$ (Fig. 1; Table 1).

The performance of the switch is very much depends on both series and shunt membranes. The membranes are designed to have same pull-in voltage to establish the optimized relation between pull-in voltage and electrostatic recovery forces. The lower spring constant is achieved by considering meandering technique for series and crab-leg structure for shunt membrane, these membranes are designed inside the cavity made up on quartz substrate. This cavity helps to restore the membranes.

When the RF input signal is applied at input port, then the series membrane has to be actuate to complete the circuit connection and shunt membrane remains in its original position offers a very low capacitance path for the transmission of signals resulting low insertion loss. Whereas in OFF state of the device, the shunt membrane is actuated and deflects the bridge vertically downwards which offers high capacitive path and at the same time series membrane retains its original position, i.e., opening the circuit to block the RF signal resulting high isolation. The gaps between electrodes are maintained at 3 and $2.5 \mu\text{m}$ for series and shunt membranes to achieve same pull-in voltage.

2.2 Capacitive/shunt switch membrane

The shunt membrane is designed with crab-leg structured meanders which are having lower spring constant and is 3.02 N/m . The circular perforations are taken in order to decrease the air squeeze film damping and the shunt membrane is shown in the Fig. 2 with dimensions.

2.3 Ohmic/series switch membrane

It is essential to design the series membrane with same pull-in voltage with the shunt membrane. Two different types of meanders are designed to reduce the spring constant which is 2.17 N/m . The inner meanders are connected with the membrane helps to maintain it uniformly without bending during actuation. The width of the membrane is exactly equal to the spliced width of the signal line such that completes the signal path in down state. The membrane and its dimensions are shown in Fig. 3.

2.4 Material selection

The material properties play a key role to increase the performance of the RF MEMS switch. Quartz is taken as the substrate material because, crystals of quartz have high resistivity of $105\text{--}108 \Omega\text{m}$ and acts as excellent insulators at elevated temperatures. Ashby's approach is used for the selection of materials for the dielectric layer and

Table 1 Device specification

S. no.	Component	Length (μm)	Width (μm)	Depth (μm)	Material
1	Substrate	412	412	200	Quartz
2	Substrate dielectric	412	412	0.5	TiO ₂
3	CPW (G/S/G)	126	31.5	1	Gold
4	Cavity	245	245	3	–
5	Series membrane	235	80	1	Gold
6	Shunt membrane	245	80	1	Gold
7	Electrode × 4	35	40	1	Gold
8	Series contact pad	35	31.5	0.5	Gold
9	Meanders width	A (10)	B (2.5)	C (3.5)	Gold
10	Signal dielectric	80	31.5	0.5	TiO ₂

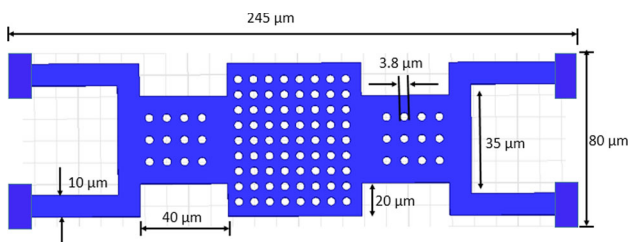


Fig. 2 Shunt membrane of proposed switch

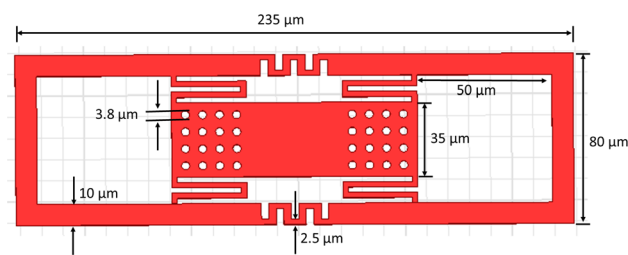


Fig. 3 Series membrane of proposed switch

membranes, in this method, at first, the materials suitable for the component are noted down and are then screened to suit the application. Then, the properties of the screened materials are studied, and, based on the parameters to be optimized, material selection charts are plotted, which gives us an unbiased picture of how the performance of the device is affected by selecting a particular material, and how the compromising effect of the parameters is reflected in the choice of materials. The significance of Ashby’s material selection approach is charts are plotted, which gives us an unbiased picture of how the performance of the device is affected by selecting a particular material, and how the compromising effect of the parameters is reflected in the choice of materials. Dielectric strength and resistivity of the dielectric layer are major parameters to enhance the performance in terms of isolation of the RF signal and charge distribution (Paldas and Gupta 2013) (Fig. 4).

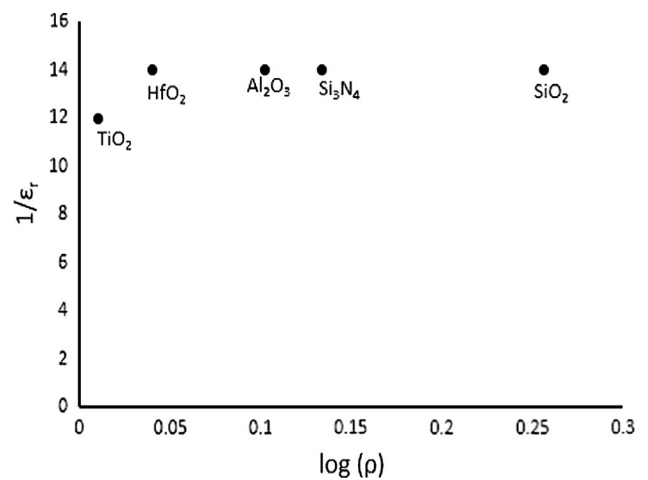


Fig. 4 Logarithmic value of resistivity vs. reciprocal of relative permittivity to select the material for dielectric layer of the switch

According to the Ashby for low pull-in voltage the value of $1/\epsilon_r$ and $\log(\rho)$ should be minimum. Hence the extreme left bottom material is the best material for the dielectric (Sharma and Gupta 2012). The TiO₂ is having the dielectric constant ($K = 100$) helps to increase the isolation in OFF state. For choosing the material for membrane young’s modulus and mass density is considered for better electromechanical performance. The operational frequency is very much dependent on the spring constant. The smaller young’s modulus of the material results in low pull-in voltage and density of the material should also be low for fast switching of the beam (Fig. 5).

\sqrt{E} value must be very small for low pull-in voltage, $\sqrt{E/\rho}$ value must be large for fast switching. Thus, Al, SiO₂ and Au are good material choices for the membrane for having low pull-in voltage. Amongst gold is preferred in this proposed structure because of high electrical conductivity.

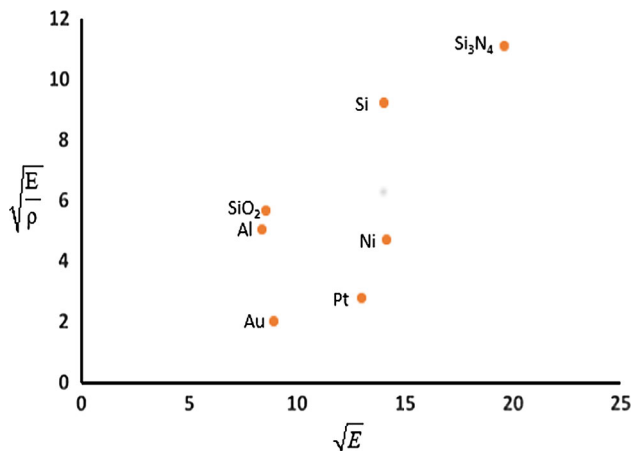


Fig. 5 Material selection for membranes of the switch

3 Fabrication flow

The fabrication process flow is similar to the standard fabrication steps where the surface micromachining technique is used to fabricate this structure.

The Fig. 6a shows the polished upper surface of the silicon substrate. A cavity is formed by etching the portion of the substrate. A mask is used to form patterns over the substrate under UV exposure and the pattern is etched 3 μm depth by the suitable etchant. The TiO₂ is deposited with 0.5 μm thickness over the substrate which acts a substrate dielectric which is shown in Fig. 6c. The Fig. 6d shows the deposition of CPW over substrate dielectric. Figure 6e shows the addition of biasing pads and electrodes. Figure 6f reports the addition of Polyimide sacrificial layer to add dielectric layer over the signal line for capacitive switch membrane followed by Fig. 6g that highlights the additional dielectric layer over the signal line. Figure 6h shows the sacrificial layer deposition to fabricate a membrane. The cut-outs are because of the exact mask used. Figure 6i shows the deposited gold material over the Polyimide sacrificial layer. At last, the sacrificial layer is removed by plasma etching or DRIE method. The suspended membrane can be seen in Fig. 6j.

4 Results and discussions

4.1 Stress distribution analysis

Finite element modeler is used to analyze various parameters of the switch such as spring constant (k), pull-in voltage etc. The analytical calculation of the spring constant is not possible for these type of complicated meander structure because till now analytical formulas are defined for simple cantilever beam, fixed—fixed beam and guided end structures [Nguyen 1998]. Hence there is a need of FEM tool in

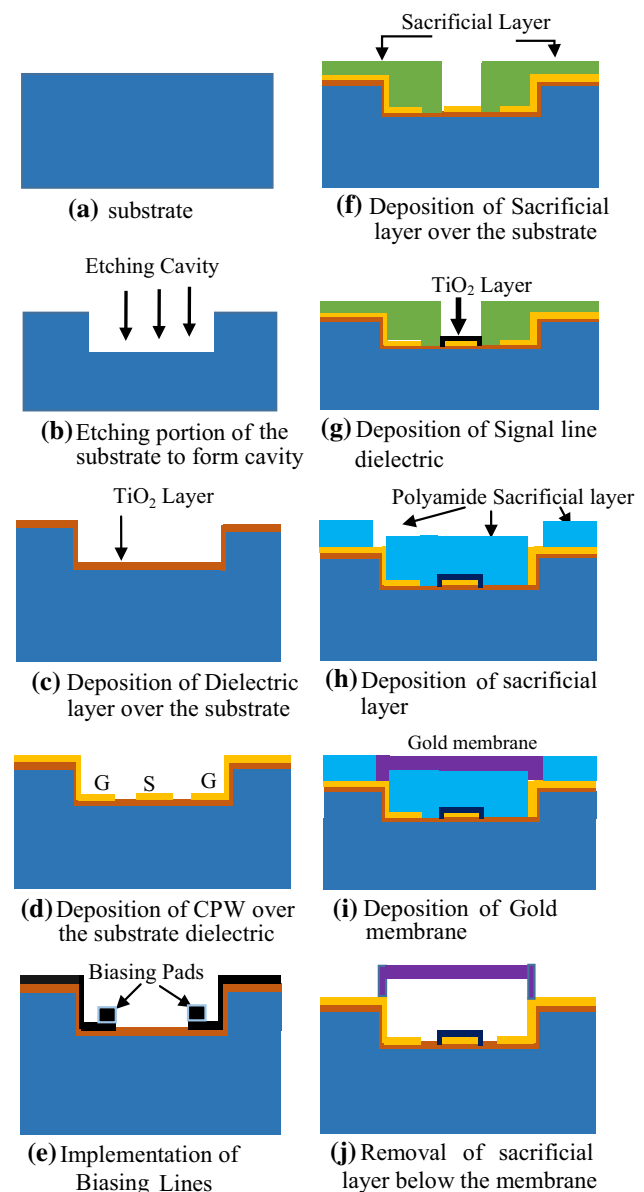


Fig. 6 Fabrication flow of proposed MEMS Switch

order to get the required parameters. So, to calculate spring constant the stress distribution need to be analyze.

The gold membrane can withstand the stress up to 100 MPa (Singh 2015). By using solid mechanics physics in COMSOL Multiphysics tool it is analyzed that maximum forced needed to produce the maximum stress of about 100 MPa, beyond this force the membrane cannot withstand and breakdown occurs (Figs. 7, 8).

It is observed that at 6.2 μN of force the series membrane is producing a stress of 99.4 MPa and at 11.6 μN the shunt membrane produces 100 MPa. Hence the maximum force required to displace the series membrane about 3 μm should be less than 6 μN and for shunt membrane about 2.5 μm should be less than 11.6 μN (Figs. 9, 10).

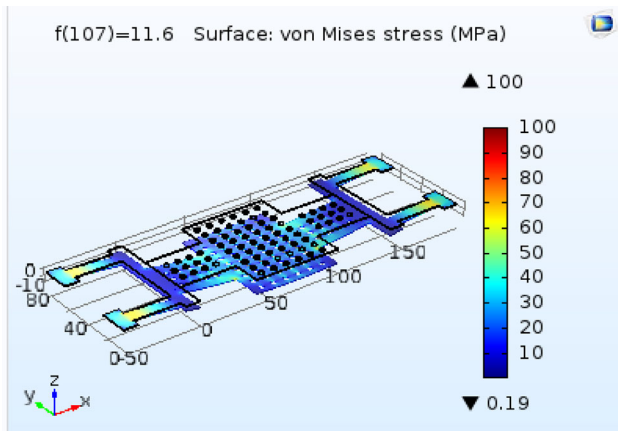


Fig. 7 Capacitive/shunt switch membrane for max. stress of 100 MPa showing maximum force of 11.6 μN

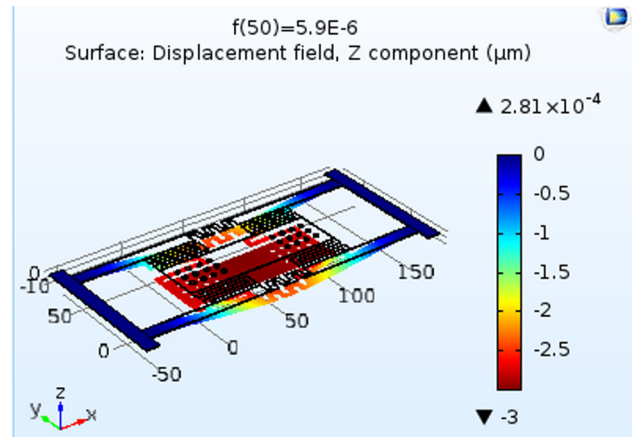


Fig. 10 Ohmic/series switch membrane for max. displacement of 3 μm showing maximum force of 5.9 μN

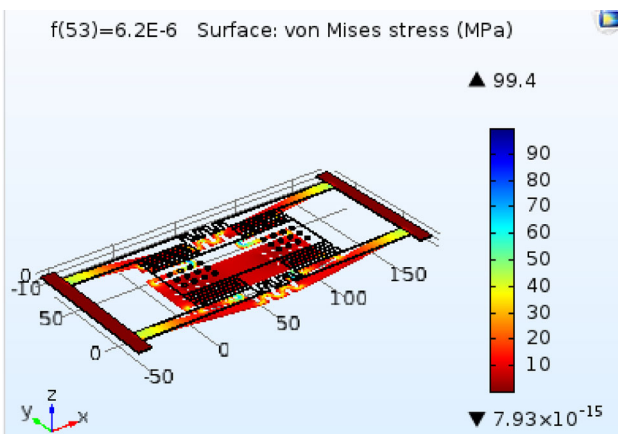


Fig. 8 Ohmic/series switch membrane for max. stress of 99.4 MPa showing maximum force of 6.2 μN

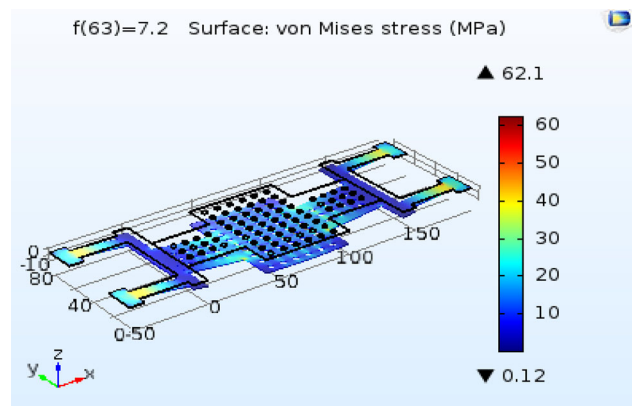


Fig. 11 Stress distribution of capacitive/shunt switch membrane at 7.2 μN of force which displaces the membrane at a displacement of 2.5 μm

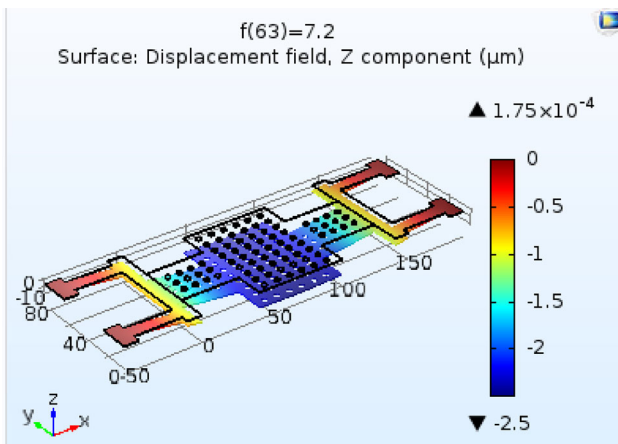


Fig. 9 Capacitive/shunt switch membrane for max. displacement of 2.5 μm showing maximum force of 7.2 μN

For series membrane and shunt membrane is simulated using FEM tool and maximum displacement of 3 μm is noted at 5.9 μN for series and 2.5 μm is noted at 7.2 μN for

shunt which are less than the maximum forces that the membranes can withstand (Figs. 11, 12).

The maximum and minimum stress distribution on the two membranes are observed by applying maximum force at which the membranes are displaced through the gap is observed as $7.34\text{E-}15$ MPa and 94.6 MPa for series membrane and 62.1 and 0.21 MPa for shunt membrane respectively. The series membrane completes the connection when it displaced at 3 μm and shunt membrane breaks the connection when it displaced 2.5 μm comes in contact with the dielectric layer.

4.2 Electromechanical analysis

4.2.1 Spring constant

The spring constant of the two switches is difficult to calculate with the analytical method because of the complicated structure of non-uniform meanders (Ravirala et al.

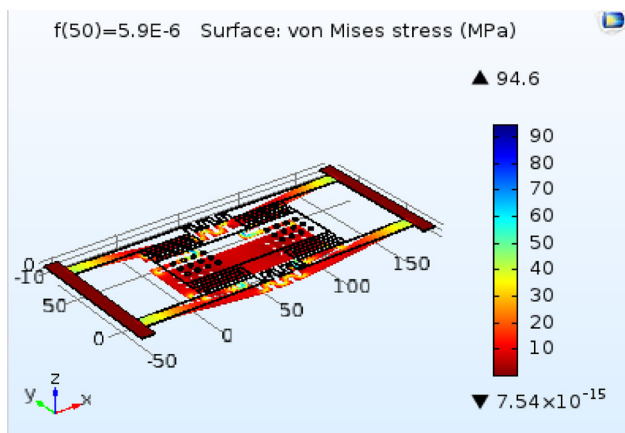


Fig. 12 Stress distribution of ohmic/series switch membrane at 5.9 μN of force which displaces the membrane at a displacement of 3 μm

2018; Singh 2015). Hence the force is applied and vertical deflection is noted to determine the spring constant of both the membranes.

According to the Newton’s Second law mass-spring-Damper system (Marcelli et al. 2010), the mechanical suspension of the spring is directly proportional to the force applied.

$$F \propto \delta \tag{1}$$

where F is applied force and δ is the deflection of the proof mass.

$$F = k\delta \tag{2}$$

$$K = F/\delta \tag{3}$$

The two membranes are simulated by applying maximum holding force of the membranes and corresponding vertical deflection is noted and ratio of those values gives

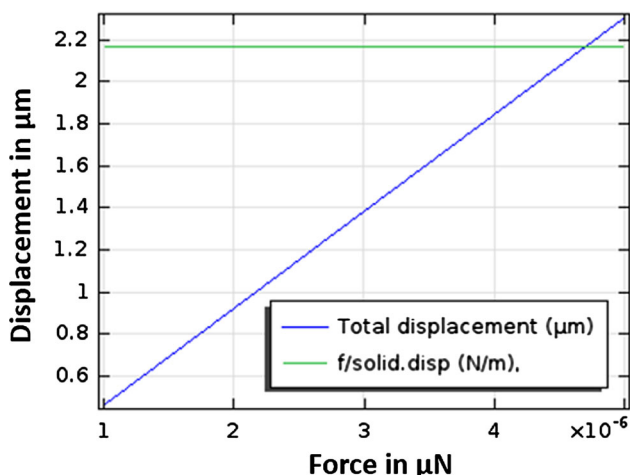


Fig. 13 Force vs. displacement showing the spring constant of series switch membrane

the spring constant of the membranes as mentioned in equation (Figs. 13, 14).

It is observed that the simulated spring constant for the series membrane is 2.17 N/m and for the shunt membrane is 3.02 N/m with the force–displacement ratio. The spring constant for the two membrane plays a key role for low pull-in voltage.

4.2.2 Pull-in voltage

The pull-in voltage of the two membranes are calculated analytically with the Eq. 4 (Rao 2017)

$$V_p = \sqrt{\frac{8kg_0^3}{27\epsilon_0 A}} \tag{4}$$

where k is the spring constant ($k = 2.17$ for series and $k = 3.02$ for shunt), $\epsilon_0 = 8.85 \times 10^{-12}$ F/m is the permittivity of the free space and A is the overlapping area of electrodes.

It is very much important to maintain the membranes at same pull-in voltage for the operation of switch. To maintain same pull-in voltage the overlapping area of series is taken as 4000 μm^2 and shunt is 3000 μm^2 . The two membranes are electrostatically actuated by applying the voltage and the electrostatic force generated is responsible for the vertical deflection of the membrane (Figs. 15, 16).

Analytically the calculated pull-in voltage for series and shunt is 22.5 V and the simulated results for series is 23.2 and for shunt is 23.5 which are close to the analytical values (Fig. 17).

The pull-in voltage is analyzed by plotting the curve between actuation voltage and vertical deflection. The above graph illustrates the series membrane displaces the

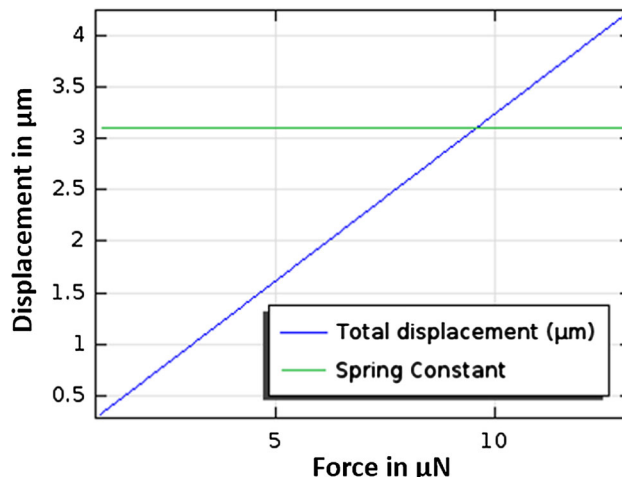


Fig. 14 Force vs. displacement showing the spring constant of shunt switch membrane

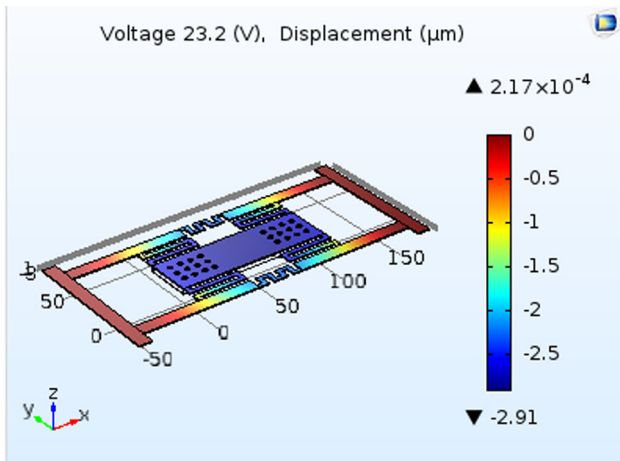


Fig. 15 Ohmic/series switch membrane at pull-in voltage of 23.2 V showing a displacement of 2.91 μm

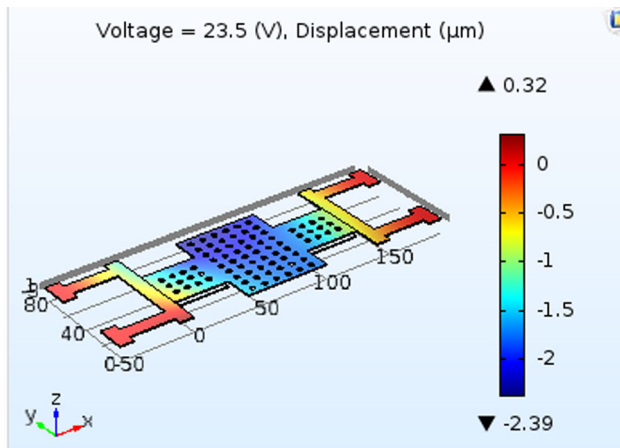


Fig. 16 Capacitive/shunt switch membrane at pull-in voltage of 23.5 V showing a displacement of 2.39 μm

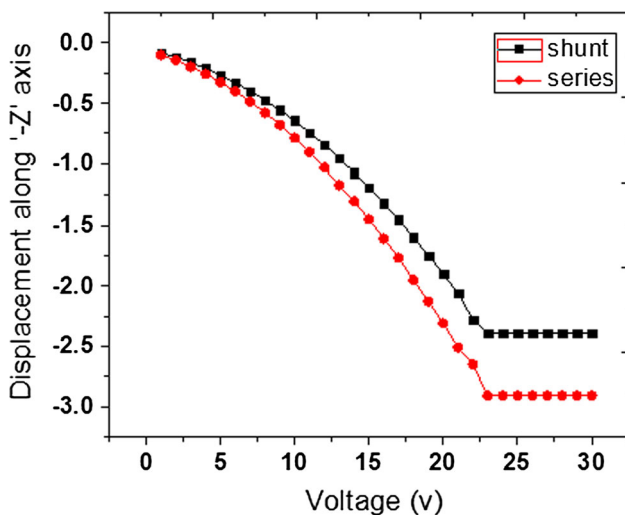


Fig. 17 Deflection analysis of both series and shunt membranes with an applied voltage

gap height 3 μm and shunt membrane displace the gap height 2.5 μm at the same voltage ($V_p = 23 \text{ V}$).

4.2.3 Up state (C_u) and down state (C_d) capacitance

Initially the device is in OFF state means the shunt membrane is actuated with voltage and is in down state and series membrane is in Up state. When the actuation voltage is applied to series membrane the membrane gets deflected to down state and at the same time the shunt membrane is not supplied with actuation voltage hence it is in upstate allowing the RF signal to pass.

The up state capacitance of the two membranes is calculated by the Eq. 5 (Lakshmi Narayana et al. 2017a, b)

$$C_{up} = \frac{(\epsilon_0 A)}{\left(g_0 + \frac{t_d}{\epsilon_r}\right)} \tag{5}$$

where, ϵ_0 is the permittivity of the free space, ϵ_r is the relative permittivity of the electrode material, A is the overlapping area between electrodes, g_0 is the gap between the electrodes and t_d is the dielectric layer thickness electrodes.

The upstate capacitance for the shunt and series membrane is calculated as 0.24 fF. The downstate capacitance can be calculated by the Eq. 6 (Fig. 18).

$$C_d = \frac{\epsilon_0 \epsilon_r A}{t_d} \tag{6}$$

The downstate capacitance of both series and shunt membrane is 14.2 fF. Hence the C_d/C_u ratio gives the capacitance sensitivity of the device and is 55.92 therefore the simulation results of capacitance of both series and shunt membrane need to be in the range of C_u-C_d (Fig. 18).

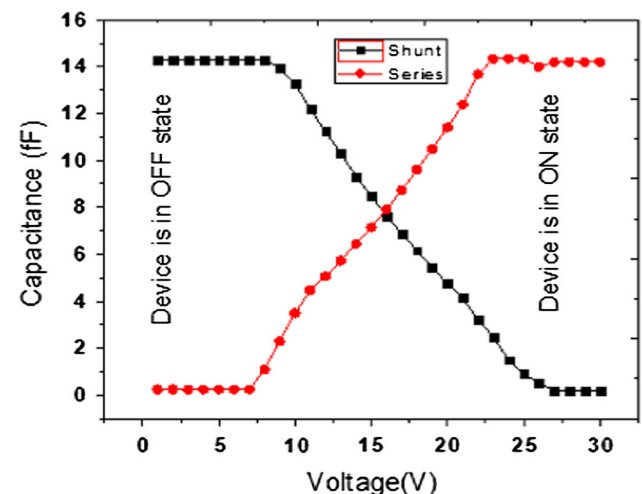


Fig. 18 Capacitance analysis of both series and shunt membranes with an applied voltage showing ON and OFF states of the switch

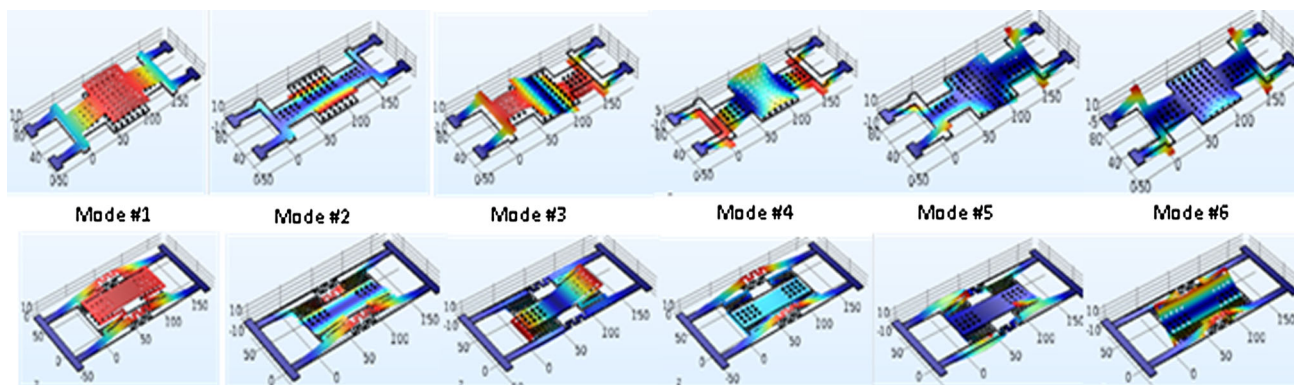


Fig. 19 Vibrating modes of both shunt and series membrane of the switch

The two membranes are simulated by applying electro-mechanics physics using comsol tool and observed the upstate capacitance of 0.24 fF and downstate capacitance of 14.2 fF and C_d/C_u ratio is 59.16.

4.3 Modal frequency analysis

Eigen frequency analysis is carried out using FEM tool conveys the information of the first six vibrating modes of the membranes are presented in the Fig. 19.

The modal frequencies is obtained by solving the Lagrangian of the system and then applying the canonical equation. The motion of the membranes under harmonic force is considered for obtaining the equation, by modelling the second order mass-spring damper system the equation of the harmonic motion of the membrane (Singh 2015) is

$$M_{ef} \frac{d^2x}{dt^2} + \gamma_{ef} \frac{dx}{dt} + kx = F_E, \tag{7}$$

where M_{ef} is the effective mass of the membrane, γ_{ef} is the effective damping coefficient of the dielectric material, F_E is the electrostatic force and k is the overall spring constant (Table 2).

Table 2 Modal frequencies of the switch

Vibrating mode	Modal frequency	
	Series membrane	Shunt membrane
Mode #1	21,615	25,490
Mode #2	37,943	62,104
Mode #3	41,715	75,929
Mode #4	67,284	141,450
Mode #5	102,890	179,940
Mode #6	110,060	214,530

The Eigen frequency analysis is carried out using COMSOL multiphysics tool to obtain the resonant frequencies of the switches. Amongst the six vibrating modes the vertical deflection mode (mode #1) is suitable for the proposed device. It is observed that the resonant frequency of the series and shunt membrane is 21.615 and 25.490 kHz, respectively. The other five vibrating modes gives uneven rise and fall of the capacitance. Hence the fluctuations in the capacitance will gives rise to the degradation of transmitting signal with the effect of noise.

4.4 Resonant frequency analysis

The resonant frequency of the switch is depends on the spring constant of the meanders and proofmass of the actuating Beam. Chakraborty et al. (2014) presented a formula to calculate the mechanical vibration of the beam has been written in Eq. (8).

$$f_0 = \frac{1}{2\pi} \sqrt{\frac{k}{m}} \tag{8}$$

where m is modal mass of the beam = $0.35 \times (L \times w \times t) \times d$. The d is density of gold = $3.55 \times 10^{-13} \text{ kg/m}^3$, $m = 118 \times 10^{-6} \text{ kg}$.

Here the proofmass and the spring constant is fixed. Hence any variation in the structure of the meanders will vary the spring constant which results in variation of frequency. The calculation of values of the frequency of shunt and series switch on the fundamental mode obtained are 21.6 and 25.49 kHz.

4.5 Switching time analysis

Switching speed of the device is considered as the utmost important factor for the performance of the device. The switching speed is also a major factor that influence the working of switch for transmit/receive applications. The

switching time is calculated by the Eq. 9 (Lakshmi Narayana et al. 2017a, b)

$$T_s = \frac{3.67V_p}{\omega_0 V_s} \tag{9}$$

where V_p is the pull-in voltage, ω_0 is the resonant frequency, V_s is the input source voltage.

The resonant frequency is determined by the spring constant and effective mass of the membrane (Singh 2015) (Fig. 20),

$$\omega_0 = \sqrt{\frac{k}{m}} \tag{10}$$

The switching response of the series membrane is 24.8 μ s and shunt membrane is 21.8 μ s hence overall switching time of the device is observed as 23.8 ns which is average of both switching times.

4.6 RF performance analysis

The performance of the switch in GHz frequency range is to be analyzed to use in RF applications. The scattering losses is analyzed by using HFSS tool.

The device contains reflection loss or return loss and insertion loss in ON state. The device is on when the shunt membrane is in upstate and series membrane is in downstate and offers very low insertion and return losses during transmission of the RF signal. During ON condition of the device return loss (S11) is the measure of impedance matching of the device (Muldavin and Rebeiz 2000a, b) and given as

$$S_{11} = \frac{-j\omega_0 C_u Z_0}{2 + j\omega C_u Z_0} \tag{11}$$

and for $S_{11} \leq -10$ dB.

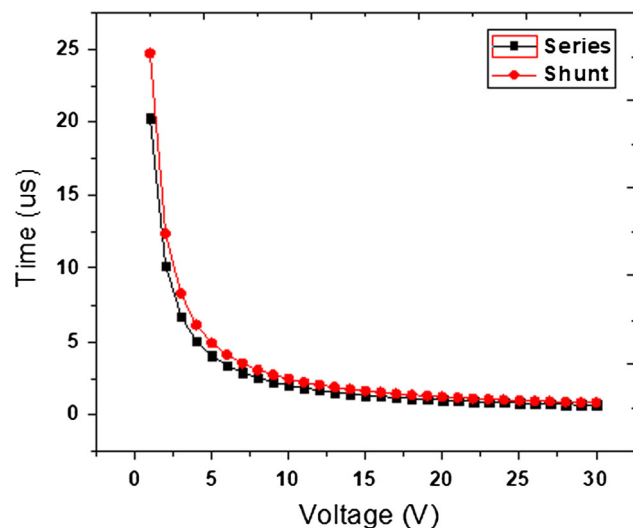


Fig. 20 Source voltage vs. switching time

$$|S_{11}|^2 \simeq \frac{\omega^2 C_u^2 Z_0^2}{4} \tag{12}$$

where ω is resonant frequency, C_u is the upstate capacitance and Z_0 is the input impedance and is taken as 50 Ω (Fig. 21).

The return loss of -59.8 dB is observed in the frequency of 5 GHz and -24.5 dB at 35 GHz.

Insertion loss is the loss of signal power resulting from the insertion of a device in a transmission line and is usually expressed in decibels (dB). Insertion loss is the loss occurs during the transmission of the RF signal. The insertion loss depend mainly on the dimensions and material of the substrate, dielectric layers and the bridge (Fig. 22).

By taking TiO_2 ($K = 100$) as a substrate dielectric the insertion loss reduced and is -0.1 dB at 5–40 GHz frequency range.

The three types of switches which are single series, single shunt and series–shunt configuration switches are simulated using HFSS tool to obtain comparison of isolation loss of switches. The isolation loss of single series and shunt switches are observed as -54 dB for single series switch at 21 GHz and -61 dB for shunt switch at 25 GHz (Figs. 23, 24).

Isolation loss of the device occurs when both the switches are in OFF state i.e., the series membrane in upstate and shunt membrane is in downstate. Hence the C_u of the series membrane and C_d of the shunt membrane plays major role in attenuating the signal (Fig. 25).

The isolation of 82.47 dB is observed at 26 GHz frequency. The switch exhibits high isolation of 82.47 dB

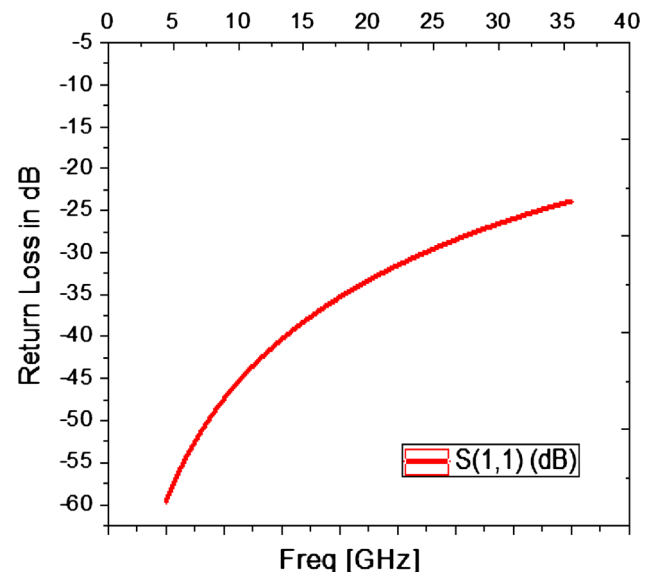


Fig. 21 Reflection loss of proposed switch at 5–40 GHz range during ON state

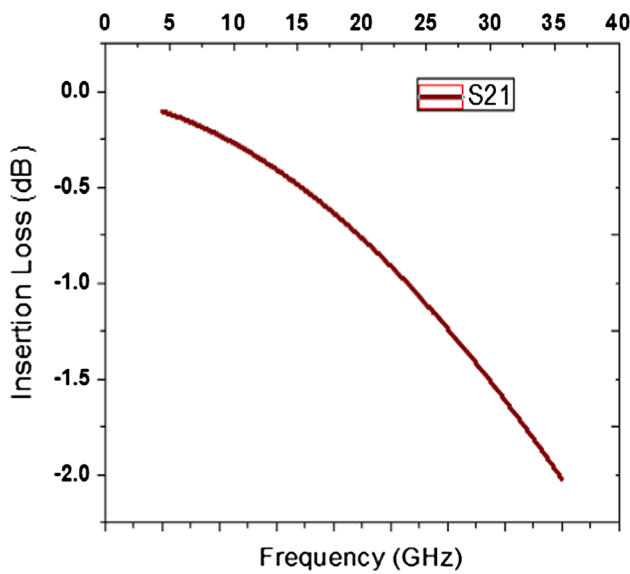


Fig. 22 Insertion loss of proposed switch at 5–40 GHz range during ON state

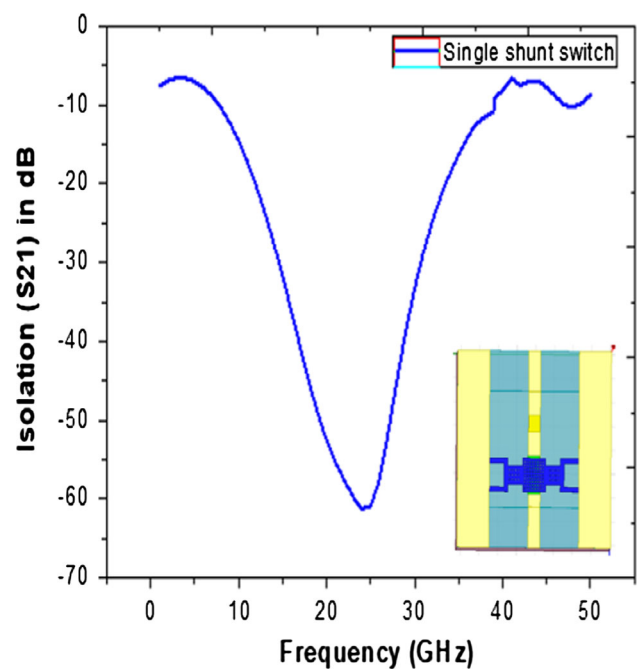


Fig. 24 Isolation loss of shunt switch at 1–50 GHz range during OFF state

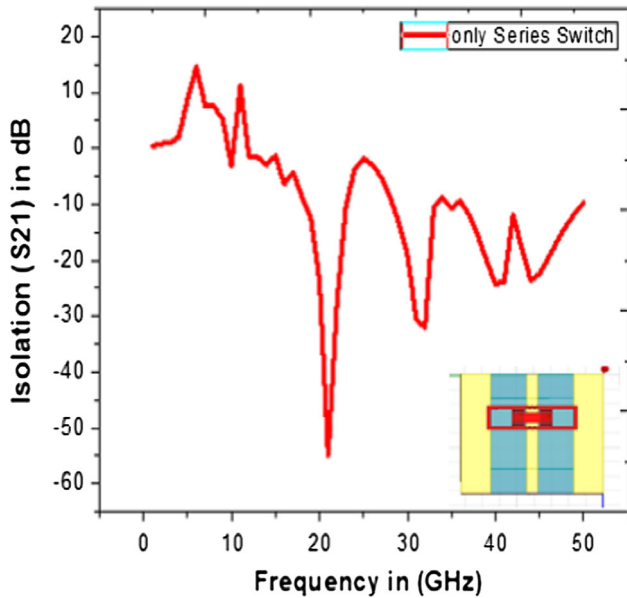


Fig. 23 Isolation loss of series switch at 1–50 GHz range during OFF state

around 26 GHz and having a bandwidth of 22 GHz typically in the range of Satellite communication applications (Table 3).

5 Conclusion

The RF MEMS switch is designed to achieve high isolation in frequency band used for satellite communication by incorporating the series and shunt membranes on the same coplanar waveguide. The two membranes are designed to

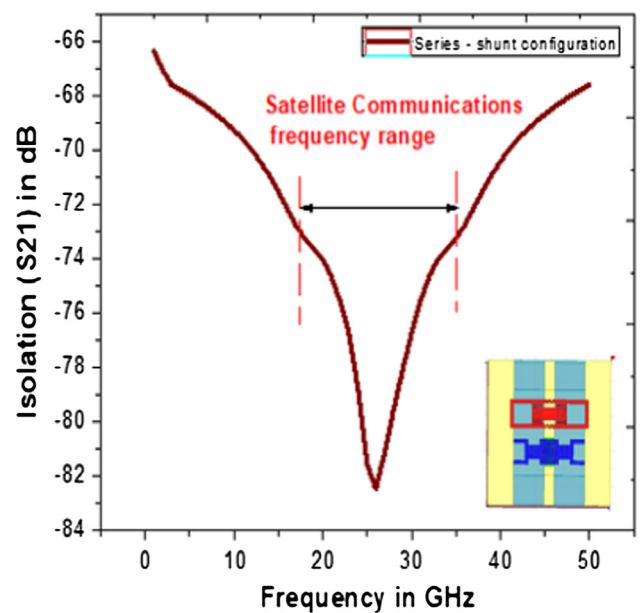


Fig. 25 Isolation loss of proposed series–shunt switch at 5–40 GHz range during OFF state

work on same actuation voltage for better performance of the switch. Low pull-in voltage is achieved by considering the meandering structured springs for the series membrane and crab-leg structured springs for the shunt membrane such that both the membranes have acceptable stress levels. The Electromechanical parameters such as pull-in voltage, spring constant, C_d , C_u , modal frequencies and RF

Table 3 Comparison of proposed switch results with existing switches

Parameter/component	Singh and Pashaie (2014)	Khaira et al. (2013)	Proposed switch
Substrate	Quartz	Silicon	Quartz
Dielectric layer	HfO ₂	HfO ₂	TiO ₂
Membrane	Gold	Gold	Gold
Electrode thickness	1.5 μm	2 μm	1 μm
Pull-in voltage	22.5 V	7.19 V	23.5 V
Switching time	–	–	23.8 ns
C _d	–	–	Theoretical: 0.27 Simulated: 0.24
C _u	–	–	Theoretical: 15.1 Simulated: 14.2
C _d /C _u ratio	–	–	Theoretical: 55.92 Simulated: 59.6
Insertion loss	< 0.1 dB	0.06	< 0.1 dB
Return loss	50 dB	14 dB	59.8 dB
Isolation loss	60 dB	72 dB	82.47 dB

performance characteristics has been analyzed in this paper. The proposed RF MEMS switch can be used in antennas of high frequency satellite communication applications where the high isolation is a major concern. The proposed series–shunt switch shows excellent isolation compared to the switches having series and shunt membranes individually with a wider bandwidth for satellite communications applications.

Acknowledgements The Authors would like to thank to NMDC supported by NPMAS, National Institute of Technology, Silchar for providing the necessary computational tools. The corresponding author (Dr. K. Srinivasa Rao) would like to thank Science Engineering research Board (SERB), Govt. of India, New Delhi (Grant File No: ECRA/2016/000757) for providing partial financial assistance to carry out the work.

Compliance with ethical standards

Conflict of interest The authors declare that they have no competing interests.

References

- Chakraborty A, Gupta B, Sarkar BK (2014) Design, fabrication and characterization of miniature RF MEMS switched capacitor based phase shifter. *Microelectron J* 45(8):1093–1102
- Daneshmand M, Faladi S, Mansour RR, Lisi M, Stajcer T (2009) Thermally-actuated latching RF MEMS switch. In: IEEE MTT-S international microwave symposium digest, pp 1217–1220
- Deng P, Wang N, Cai F et al (2017) A high-force and high isolation metal-contact RF MEMS switch. *Microsyst Technol* 23:4699. <https://doi.org/10.1007/s00542-017-3302-3>
- Ilkhechi AK, Mirzajani H, Aghdam EN et al (2017) A new electrostatically actuated rotary three-state DC-contact RF MEMS switch for antenna switch applications. *Microsyst Technol* 23:231. <https://doi.org/10.1007/s00542-015-2714-1>

- Khaira NK, Singh T, Sengar JS (2013) Stress analysis using finite element modeling of a novel RF microelectromechanical system shunt switch designed on quartz substrate for low-voltage applications. *Trans Electr Electron Mater* 14(5):225–230
- Lakshmi Narayana T, Girija Sravani K, Srinivasa Rao K (2017a) Design and analysis of CPW based shunt capacitive RF MEMS switch. *Cogent Eng*. <https://doi.org/10.1080/23311916.2017.1363356>
- Lakshmi Narayana T, Girija Sravani K, Srinivasa Rao K (2017b) A micro level electrostatically actuated cantilever and metal contact based series RF MEMS switch for multi-band applications. *Cogent Eng*. <https://doi.org/10.1080/23311916.2017.1323367>
- Lee HC, Park JH, Park JY, Nam HJ, Bu JU (2009) Design, fabrication and RF performance of two different types of piezoelectrically actuated ohmic MEMS switches. *J Micromech Microeng* 15(11):2098–2104
- Marcelli R, Lucibello A, De Angelis G, Proietti E, Comastri D (2010) Mechanical modelling of capacitive RF MEMS shunt switches. *Microsyst Technol* 16:1057–1064. <https://doi.org/10.1007/s00542-009-1007-y>
- Muldavin JB, Rebeiz GM (2000a) High-isolation CPW MEMS shunt switches, part 1: modeling. *IEEE Trans Microw Theory Tech* 48(6):1045–1052
- Muldavin JB, Rebeiz GM (2000b) High-isolation CPW MEMS switches: part 2: design. *IEEE Trans Micro Tech* 48(6):1053–1056
- Nguyen CTC (1998) Microelectromechanical devices for wireless communications. In: The 11th annual international workshop on micro-electro-mechanical-systems, Heidelberg, Germany, pp 1–7
- Pacheco SP, Katehi LP, Nguyen CTC (2000) Design of low actuation voltage RF MEMS switch. In: IEEE MTT-S international microwave symposium digest, vol 1. Boston, pp 165–168
- Paldas A, Gupta N (2013) Material selection and parameter characterization for RF MEMS switches. *Int J Mech Prod Eng* 1(3):7–12
- Ravirala AK, Srinivasa Rao K et al (2018) Design and performance analysis of uniform meander structured RF MEMS capacitive shunt switch along with perforations. *Microsyst Technol* 24(2):901–908. <https://doi.org/10.1007/s00542-017-3403-z>

- Rebeiz GM (2003) RF MEMS: theory, design, and technology, 1st edn. Wiley, New York
- Ruan M, Shen J, Wheeler CB (2001) Latching micromagnetic relays with microstrip permalloy cantilevers. In: The 14th IEEE international conference on micro electro mechanical systems, vol 1. Interlaken, Switzerland, pp 224–227
- Sharma AK, Gupta N (2012) Material selection of RF-MEMS switch used for reconfigurable antenna using Ashby's methodology progress. *Electromag Res Lett* 31:147–157
- Singh T (2015) Design and finite element modeling of series-shunt configuration based RF MEMS switch for high isolation operation in K-Ka band. *J Comput Electron* 14(1):167–179. <https://doi.org/10.1007/s10825-014-0636-2>
- Singh T, Pashaie F (2014) Circuit modelling and Eigen frequency analysis of a poly-si based RFMEMS switch designed and modelled for IEEE 802.11ad protocol. *J Comput Sci Eng* 8(3):129–136
- Yao ZJ, Chen S, Eshelman S, Denniston D, Goldsmith CL (1999) Micromachined low-loss microwave switches. *IEEE J Microelectromech Syst* 8(2):129–134
- Zolfaghari P, Arzhang V, Zolfaghari M (2018) *Microsyst Technol.* <https://doi.org/10.1007/s00542-017-3684-2>

Publisher's Note

Springer Nature remains neutral with regard to jurisdictional claims in published maps and institutional affiliations.